Platelet margination dynamics in blood flow: The role of lift forces and red blood cells aggregation

Mariam Dynar, Hamid Ez-Zahraouy, Chaouqi Misbah, Mehdi Abbasi

Platelet margination dynamics in blood flow: the role of lift forces and red blood cells aggregation

Mariam Dynar,[1,*] Hamid Ez-Zahraouy,[2] Chaouqi Misbah,[1,†] and Mehdi Abbasi[3,‡]

[1] *Université Grenoble Alpes, CNRS, LIPhy, F-38000 Grenoble, France*
[2] *Laboratoire de Matire Condense et Sciences Interdisciplinares, URL-CNRST, Mohammed V University in Rabat, Morocco*
[3] *Aix Marseille Univ, CNRS, CINAM, Turing Centre for Living Systems, Marseille, France*

Homeostasis plays a critical role in maintaining the delicate balance between preventing excessive bleeding and enabling clot formation during injuries. One pivotal aspect of homeostasis involves the development of platelet clots. In this study, we analyze numerically the behavior of platelet margination as a function of the adhesion energy between red blood cells (RBCs), driven by the presence of plasma proteins. We examine scenarios encompassing both physiological conditions and pathological states, such as those seen in patients with diabetes. Employing a two-dimensional simulation (2D), we utilize rigid particles and a vesicle model to simulate platelets and RBCs, respectively. We employ the Lattice Boltzmann method (LBM) to solve the underlying model equations. We first demonstrate that platelet margination is primarily determined by lift forces and is not notably affected by whether the cells undergo tank-treading (TT) or tumbling (TB), as often reported. Specifically, we unveil instances where cells exhibit TT or TB behavior, yet their platelet concentration profiles closely resemble each other. Furthermore, we present a striking result concerning the impact of RBC adhesion. In microcirculation the hematocrit is in the range of 5-20%. A moderate adhesion energy (falling within the physiological range), boosts platelet margination in microcirculation. However, this effect becomes small for larger hematocrit encountered in macrocirculation (e.g. 40 %). This boost is more significant for a viscosity contrast (viscosity of cytoplasm over that the suspending fluid) equal to a known value for RBC, as compared to the case without viscosity contrast. As we increase the adhesion energy (the pathological range), a noteworthy decline in platelet margination is found, albeit that for some flow strength the platelet margination reaches a minimum and increases again at higher adhesion energy. These results can be attributed to a combination of lift generated by the bounding walls and the formation of RBC clusters. Notably, our study sheds light on a critical consequence of excessive adhesiontypically observed in pathological conditions like diabetes mellitus.

* mariam.dynar@univ-grenoble-alpes.fr
† chaouqi.misbah@univ-grenoble-alpes.fr
‡ mehdi1abbasi@gmail.com

I. INTRODUCTION

Red blood cells (RBCs) are essential for the delivery of oxygen and nutrients to tissues and organs. RBCs are the predominant blood cells, they occupy about 45% of the total blood volume, while plasma occupies about 55% and other cells (platelets, white cells) less than 1%. The permanent mutual interaction between RBCs and vessel walls as well as among RBCs dictate the overall blood flow properties. Platelets -Thrombocytes- are the smallest blood cells in the human body. Their number is approximately 150.10^9 platelets per liter, and their diameter is between $2\mu m$ and $4\mu m$ (significantly smaller than RBC diameter which is about $8\mu m$) [59]. The main functions of platelets are to recognize and repair damaged endothelium (monolayer of endothelial cells lining the internal surface of blood vessels)[61]. This monolayer of cells is responsible for the control of vascular permeability and intervenes in immune responses at places of infection or injury [51]. Another important role of platelets is to activate the process of blood clotting to stop bleeding[30]. More precisely, blood clotting in this process consists of a platelet-plug formation, and is the most important step in homeostasis (process of stopping bleeding due to an injury).

An important question, regarding platelets, which has been thoroughly addressed in the literature pertains to their margination by RBCs: RBCs have a tendency to push platelets towards the vessel periphery [11, 54, 60]. If this is the case in-vivo, this effect would mean that platelets are often located close to vessel walls and ready to initiate homeostasis in case of an injury, or to contribute, via a complex pathway, to repairing damaged endothelium.

Before describing the main focus of the present work, let us first recall the main results regarding margination of platelets. Under physiological conditions, platelets tend to move toward vessel walls, this phenomena is called platelets margination [54]. It is known that the platelet's margination rate is affected by the shape and the size of platelets [11, 54]. Unactivated platelets can be considered as rigid discoidal particles. Activated platelets change their shape from a discoid shape to a spherical shape. This shape change is caused by the contact between platelets and endothelial cells or by their exposure to circulating agonists [43]. According to in vitro study, platelet margination is caused by the hydrodynamic interaction between RBCs and platelets [11, 60]. Moreover, RBCs properties may impact the platelet margination. In a numerical study, Danviel et al [54] modeled RBCs and platelets flow in three dimension using lattice Boltzmann method (LBM), and found that the increase of RBCs deformability as well as the increase of the hematocrit enhance platelet margination. They also reported that the inner viscosity of RBCs affects inversely the platelet margination [54]. Furthermore, it has been shown that there exists an optimal wall shear rate value corresponding to maximum of the platelet's margination rate [30, 35]. Moreover, it has been reported that this critical shear rate value depends on the tube diameter[30]. Besides platelet margination, margination of white blood cells[17, 18, 21, 40] as well as rigid RBCs have also been studied[45].

Many studies on platelet margination by RBCs have been based on numerical simulations [5, 11, 30, 35, 49, 52–54, 62, 64] or on in-vitro experimental studies[1, 14, 16, 56, 60], and focused on physiologically-inspired situations. There are, however, several pathological situations which have not been yet addressed. One typical example is the case where RBCs form more or less robust aggregates. Under physiological conditions, aggregates are reversible, that is, they form and they dissociate in the course of time. There are pathological situations where aggregate can form in an irreversible way. It is known, for example, that patients suffering from diabetes can have robust aggregates that may even lead to blood occlusions in microcirculation [20]. Our aim here is to analyze platelet margination in the presence of RBC aggregates. Fibrinogen is believed to be the main protein responsible for RBCS aggregates formation. It is often reported that fibrinogen within diabetic patients has higher concentrations $(6,56 \pm 1,30 mg/ml)$ than normal range $(3,24 \pm 1,39 mg/ml)$ [6], a fact that can enhance aggregation.

In the present work, we analyze systematically the platelet margination process by means of 2D simulation in the presence of RBCs aggregation. Our simulations consists of a confined binary suspension of rigid particles and deformable 2D particles (vesicles, a widely adopted simple model for RBCs) mimicking platelet and RBCs respectively. We find that, when the adhesion force between RBCs is not too strong, the platelet margination is boosted for hematocrits relevant to microcirculation (lying in the range 5-20%[7, 29, 34, 38]). However, for higher hematocrits the effect is less pronounced. For a high enough adhesion energy (mimicking pathological situations), the RBCs tend to form stable aggregates. This leads to a reduction of platelet margination, but for some flow strengths we observe a second increase of margination at high adhesion energies. In order to dig further into the link between adhesion force and the platelet margination, we explore the behavior of cell free layer as a function of the adhesion energy between RBCs and we find that the cell free layer thickness decreases upon increasing the adhesion energy between RBCs. Finally, we analyze the role of viscosity contrast. When the viscosity contrast is high enough, we find a decrease in the margination. Contrary to previous claims[30, 54], it is not the decrease of tank-treading of the membrane (which is reduced upon increasing the viscosity contrast) which reduces directly the margination, but it is rather an indirect effect: the transverse migration (or lift) of RBCs is reduced due to an increase of viscosity contrast , and this leads, in turn, to a decline of the margination effect.

II. METHODOLOGY

Two dimensional simulations (2D) are performed to carry out our study. The simulation is based on Lattice-Boltzmann method (LBM). The 2D model was selected for computational efficiency. In 2D simulation, the membrane is considered as a contour instead of a surface. It has been reported that 2D model captures many shapes and phenomena observed in three dimensions. Indeed, the parachute and slipper shapes[22, 23], multilobe shape[3, 33, 42] are observed both in 2D and 3D. In addition, the shapes of aggregated RBCs doublets at equilibrium [19] share strong similarity between 2D and 3D. In addition, the phase diagram (in the plane of flow strength and adhesion energy) of the aggregates (a topic of the present study) obtained in 2D is quite similar to that found in 3D[2].

RBCs and platelets are modeled here by 2D vesicles and rigid particles respectively. A suspension of vesicles and rigid particles is set in a straight channel of length L and width W. A long enough tube is needed to simulate the process of margination (A tube length of about $330\mu m$ was necessary), due to the length and time scales necessary for the margination process to show up in a significant manner[54]. The suspension is subjected to a Poiseuille flow, by applying a body force in the LBM, briefly recalled below. The schematic of the system is illustrated in Fig. 1.

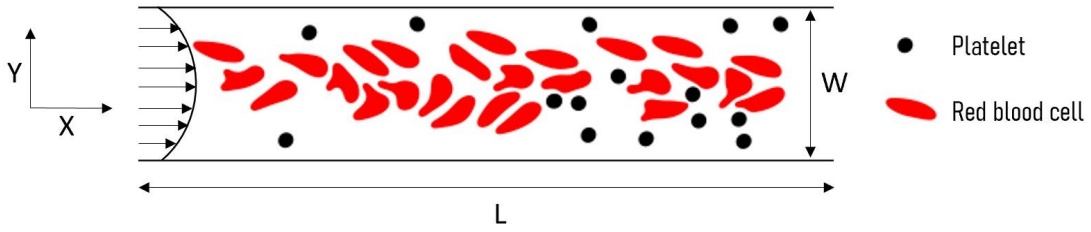

FIG. 1. Binary suspensions of RBCs and platelets under parabolic flow.

The imposed velocity (in the absence of cells) along x and y axes reads:

$$\begin{aligned} U_x &= \frac{4U_{max}}{W^2}(Wy - y^2), \\ U_y &= 0, \end{aligned} \tag{1}$$

where U_{max} is the maximum velocity, which is attained at the center line located at $y = \frac{W}{2}$. The total flow field (the imposed one and that induced by the presence of the cells) of internal and external fluids obeys the Navier-Stokes (NS) equations:

$$\rho\left(\frac{\partial \mathbf{u}}{\partial t} + \mathbf{u}.\nabla\mathbf{u}\right) = -\nabla p + \eta\nabla^2\mathbf{u} + \mathbf{f}, \tag{2}$$

$$\nabla.\mathbf{u} = 0, \tag{3}$$

where ρ,$\mathbf{u}$ and p are respectively the density, velocity and pressure. η is the viscosity of the fluid, where η=η_{in} will denote the viscosity of the fluid inside the vesicles and η=η_{ex} that of suspending fluid. $\mathbf{f}$ is the force applied by the vesicle on the fluid, to be specified below.

The membrane energy contains three contributions, the bending energy, the membrane incompressiblity condition [65], and the adhesion energy between all vesicles (which will be modeled by a Lennard-Jones potential). The cell membrane is indicated by Γ. In 2D, the energy of the membrane is given by :

$$E = \sum_i E_i^b + \sum_{i \neq j} E_{i,j}^{adh}, \tag{4}$$

where

$$E_i^b = \frac{k}{2}\oint_{\Gamma_i} c^2 ds + \oint_{\Gamma_i} \zeta ds \tag{5}$$

is both the bending and incompressibility energy of the ith vesicle, and

$$E_{i,j}^{adh} = \varepsilon_0 \oint_{\Gamma_i} ds(\mathbf{m}_i) \oint_{\Gamma_j} ds(\mathbf{m}_j)\phi(|\mathbf{m}_i - \mathbf{m}_j|). \tag{6}$$

is the adhesion energy between the ith and jth vesicles. ds corresponds to the distance between two adjacent membrane points, c and k are respectively the local curvature of the membrane and the membrane bending rigidity (taken to be $k = 4.10^{-19}J$), ζ is a local Lagrange multiplier associated with the constraint of local perimeter inextensibility, $\phi = -2(\frac{h}{r_{ij}})^6+(\frac{h}{r_{ij}})^{12}$ is the Lennard-Jones potential which describes attractive interaction at long ranges and repulsive interaction at short ranges. h is the equilibrium distance between two different points located on two different vesicles i and j. In the literature[12], it has been reported that the intercellular distance is about 25 nm for RBCs in plasma. In our simulation, due to a compromise between computational time and spatial resolution, we have set $h = 400$ nm. The chosen distance ensures a good agreement between simulation and experiments, as reported in previous studies[8, 13, 19]. ε_0 is the minimum energy associated to this distance. $\mathbf{r}_{ij} = \mathbf{m}_i - \mathbf{m}_j$, is the vector between two points setting on two different vesicle membranes, where $\mathbf{m}_i$ and $\mathbf{m}_j$ are the two position vectors of the two points of the ith and jth vesicles.

Before proceeding further, a remark is in order. Neu and Meiselman[46] proposed initially a quite involved model for interaction energy between RBCs. Their model was successfully confronted with experimental data [10]. It has also be shown that the Neu and Meiselman model can be well approximated by a Morse potential[39], which is well approximated by a Lennard-Jones potential[37]. Other experimental data based on AFM measurement seem consistent with a Lennard-Jones like potential[57], albeit no systematic attempt was made there.

The membrane force can be obtained by the functional derivative of the energy Eq. (4). The total membrane force is expressed as:

$$\mathbf{F}(\mathbf{m}_i) = \mathbf{F}^b(\mathbf{m}_i) + \mathbf{F}^{adh}(\mathbf{m}_i), \tag{7}$$

where

$$\mathbf{F}^b(\mathbf{m}_i) = k\left[\frac{\partial^2 c}{\partial s^2} + \frac{c^3}{2}\right]\mathbf{n} - c\zeta\mathbf{n} + \frac{\partial \zeta}{\partial s}\mathbf{t} \tag{8}$$

is the functional derivative of the bending energy supplemented with the membrane incompressibility condition, $\mathbf{n}$ and $\mathbf{t}$ are respectively the normal and tangential unit vector. More details can be found in reference [28].

The adhesion force takes the form

$$\mathbf{F}^{adh}(\mathbf{m}_i) = -\varepsilon_0 \sum_{j\neq i} \int_{\Gamma_j} \left[\frac{d\phi(r_{ij})}{dr_{ij}}\left(\frac{\mathbf{r}_{ij}}{r_{ij}}.\mathbf{n}(\mathbf{m}_i)\right) + c(\mathbf{m}_i)\phi(r_{ij})\right]\mathbf{n}(\mathbf{m}_i)ds(\mathbf{m}_j), \tag{9}$$

obtained by the functional derivative of the adhesion energy between ith and jth vesicles.

The dimensionless form of the forces can be written as:

$$\bar{\mathbf{F}}^b(\mathbf{m}_i) = \left[\frac{\partial^2 \bar{c}}{\partial \bar{s}^2} + \frac{\bar{c}^3}{2}\right]\mathbf{n} - \bar{c}\bar{\zeta}\mathbf{n} + \frac{\partial \bar{\zeta}}{\partial \bar{s}}\mathbf{t}, \tag{10}$$

and

$$\bar{\mathbf{F}}^{adh}(\mathbf{m}_i) = -\bar{\varepsilon}_0 \sum_{j\neq i} \int_{\Gamma_j} \left[\frac{d\bar{\phi}(\bar{r}_{ij})}{d\bar{r}_{ij}}\left(\frac{\bar{\mathbf{r}}_{ij}}{\bar{r}_{ij}}.\mathbf{n}(\mathbf{m}_i)\right) + \bar{c}(\mathbf{m}_i)\bar{\phi}(\bar{r}_{ij})\right]\mathbf{n}(\mathbf{m}_i)d\bar{s}(\mathbf{m}_j). \tag{11}$$

The dimensionless variables are defined as follows:

$$\bar{F} = \frac{R_0^3 F}{k}, \quad \bar{\varepsilon}_0 = \frac{R_0^3 \varepsilon_0}{k}, \quad \bar{c} = cR_0, \quad \bar{s} = \frac{s}{R_0}, \quad \bar{r}_{ij} = \frac{r_{ij}}{R_0}, \quad \bar{\phi}(\bar{r}_{ij}) = \phi(\bar{r}_{ij}R_0). \tag{12}$$

Let us recall that ε_0 is the minimal energy between two points belonging to two different vesicles. In fact, the adhesion energy between two planes (like when two vesicles adhere to each other with a straight shape in the adhered region), the minimal energy is different from ε_0, denoted as ε, and is equal to [2] :

$$\varepsilon = 1.6862h\varepsilon_0 \tag{13}$$

In the spirit of LBM, the force acting on the membrane is treated in an immersed sense la Peskin [50]. The force action is defined in the 2D domain (not only at the membrane). For any given point of coordinate $\mathbf{r}$ of the fluid domain we define the force as

$$\mathbf{f}(\mathbf{r}) = \int_\Gamma \mathbf{F}(\mathbf{m}_i)\delta^{2D}(\mathbf{r} - \mathbf{m}_i)ds \tag{14}$$

Where δ^{2D} is the 2D smeared Dirac function. More details about the mathematical model can be found in [55] .

A. Lattice-Boltzmann Method (LBM)

Fluid flow simulation is performed using the Lattice Boltzmann Method (LBM). In LBM, the fluid is considered as a set of pseudo-fluid particles, which can collide with each other and propagate. The spatial position and the velocity of pseudo-particles are discretized. This means that every pseudo-particle is allowed to move just along specific directions with given discrete speeds.

A distribution function $f_i(\mathbf{r},t)$ is associated with each single pseudo-fluid-particle. $f_i(\mathbf{r},t)$ gives the probability of finding the pseudo-fluid-particle at time t, at position $\mathbf{r}$ (the discrete lattice nodes position vector) having velocity c_i in the i-direction. The time evolution of $f_i(\mathbf{r},t)$ is governed by the Boltzmann equation (composed of streaming operation (left) and collision (right) operation) expressed as:

$$f_i(\mathbf{r}+\mathbf{c}_i,t+1) - f_i(\mathbf{r},t) = -\frac{1}{\tau}[\, f_i(\mathbf{r},t) - f_i^{(0)}(\mathbf{r},t)], \tag{15}$$

where τ is the relaxation time and $f_i^{(0)}(\mathbf{r},t)$ is the equilibrium distribution obtained from an approximation of the Maxwell-Boltzmann distribution. In this study, we use the D2Q9 lattice, where D2 stands for two-dimensional space and Q9 represents the total number of discrete allowed velocity vectors. The hydrodynamical macroscopic quantities describing the flow are given by: (i) the local mass density $\rho(\mathbf{r},t) = \sum_{i=0}^{8} f_i(\mathbf{r},t)$, (ii) the local fluid velocity $\mathbf{u}(\mathbf{r},t) = \dfrac{1}{\rho(\mathbf{r},t)} \sum_{i=0}^{8} f_i(\mathbf{r},t)\mathbf{c}_i$ and (iii) the local fluid pressure $p(\mathbf{r},t) = \rho(\mathbf{r},t)c_s^2$ ($c_s = 1/\sqrt{3}$ is the lattice speed of sound). In order to impose a Poiseuille flow, a constant term, F_i, representing a volumic force, is added on the right hand side of (15). Further details on this issue, and in general on the LBM can be found in references [25, 26, 32].

B. Dimensionless parameters

Several dimensionless parameters enter our problem (Dimensionless parameters are calculated relative to RBC dimensions and characteristics):

- The Reynolds number:

$$R_e = \frac{\rho\dot{\gamma}R_0^2}{\eta_{ex}} \tag{16}$$

- The capillary number, which quantifies the flow strength over bending rigidity of the membrane (in our study, we maintained the capillary number within the range of 30 to 70, which corresponds to shear rate values ranging from $550s^{-1}$ to $1000s^{-1}$ measured in the arterioles):

$$C_a = \frac{\eta_{ex}\dot{\gamma}R_0^3}{k} = \tau_c\dot{\gamma}, \tag{17}$$

  where $\tau_c = \eta_{ex}R_0^3/k$ is the shape relaxation time of the vesicle.

- The confinement which describes the ratio between effective vesicle diameter and channel width:

$$C_n = \frac{2R_0}{W} \tag{18}$$

- The viscosity contrast, which is the ratio between the viscosities of internal η_{in} and external η_{ex} fluids:

$$\lambda = \frac{\eta_{in}}{\eta_{ex}} \tag{19}$$

- The reduced area which combine the vesicle perimeter P and its enclosed area A:

$$\tau = \frac{4A\pi}{P^2} \tag{20}$$

  $\tau = 1$ for a circle, and is less than unity for any other shape.

- The Hematocrit, which refers to the total area percentage of RBCs within the channel:

$$\phi(\%) = \frac{nA}{WL} * 100, \tag{21}$$

  where n is the number of cells within the computation domain.

- The dimensionless macroscopic adhesion energy, which is defined as:

$$\bar{\varepsilon} = \frac{\varepsilon R_0^2}{k}, \tag{22}$$

where k is the bending rigidity of the membrane (taken to be $k = 4.10^{-19} J$), R_0 taken to be $R_0 = 3\,\mu m$, is the effective vesicle radius, $\dot{\gamma}$ is the applied shear rate, W is the channel width and ε is the adhesion energy between two vesicles (directly related to the concentration of fibrinogen [8]). The interaction energy between two RBCs was quantified using single cell force microscopy at various fibrinogen and Dextran levels by Brust et al [8]. Table I summarizes their results. From Table I,we can estimate which range of protein level corresponds to our simulation condition and whether our condition is physiological or pathological.

TABLE I. Fibrinogen concentration and their associated interaction energy and dimensionless macroscopic adhesion energy [8]. Physiological values are indicated with blue color, pathological values with red color and intermediate state with orange color.

Fibrinogen concentration (mg/ml)	0.898	2.391	4.197	5.402	6.597	8.098
Interaction energy $(\mu\, J/m^2)$	1.884	2.719	3.748	4.655	4.922	−6.566
Dimensionless macroscopic adhesion energy $\bar{\varepsilon}$	42.38	61.17	84.33	104.73	110.74	147.73

The Lattice Boltzmann Method (LBM) by using the Immersed Boundary Method (IBM) were adopted to perform our 2D simulation [31, 32]. The Reynolds number is set to $R_e = 0.1$, which is a value that ensures a good balance between numerical efficiency and good precision for the Stokes regime [58]. The value of the reduced area is set to $\tau = 0.64$ for RBC (This value provides a biconcave equilibrium shape and inspired by that of human RBCs) and $\tau = 1$ for platelets (a circular shape). The confinement value was set to $C_n = 0.2$ during simulation. Table II presents the simulation parameters used in this article.

III. RESULTS

In this section we present the main results by analyzing the effects of the three main parameters: i) Capillary number, ii) viscosity contrast, and iii) adhesion energy.

TABLE II. Simulation parameters inspired from human RBCs.

Parameters	Physical unit
R_0	$3\mu m$
η_{ex}	$1mPa\,s$
k	$4.10^{-19} J$
τ_c	$0.067s$

A. The effect of the capillary number on platelet margination

The present subsection is dedicated to the examination of how the capillary number affects the platelets distributions near walls. For that purpose, we performed simulations of RBCs and platelets flowing through two channels of different confinements $C_n = 0.2, 0.4$ (corresponding channel widths $D = 15\mu m, 30\mu m$, respectively). Once the particles are prepared inside the channel, we applied a parabolic flow with different capillary numbers $C_a = 5, 30, 70$, these values are in the wall shear rate range of arterioles and venules.

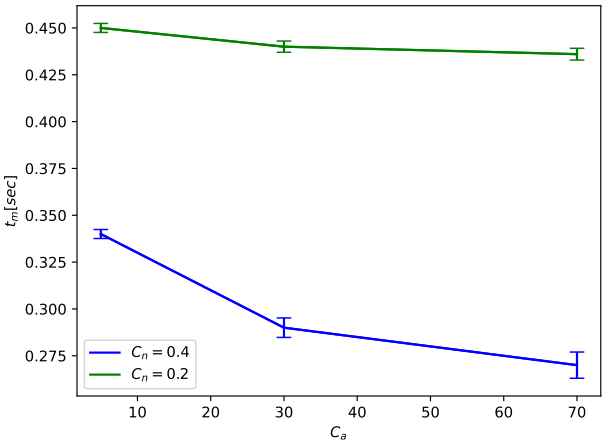

FIG. 2. The average time needed by a half of platelets to reach the cell free layer for $C_n = 0.2, 0.4$ as a function of C_a.

Figure 2 presents the average time needed by a half of platelets to reach the cell free layer (CFL). Figure 2 shows that the increase of the capillary number from $Ca = 5$ to $Ca = 70$ in case of $C_n = 0.2$ does not affect the margination. In contrast, for a confinement $C_n = 0.4$ platelets spend less time to reach the CFL (Cell Free Layer). Moreover, increasing the capillary number, the platelets need less time to reach the CFL.

Figure 3 shows the local concentration averaged over time of platelets (ϕ_{plt}) and of RBCs (ϕ_{RBCs}) in the channel. For confinement $C_n = 0.2$ (Fig. 3(a)), the increase of shear rate does not affect the margination. In contrast, when $C_n = 0.4$, margination becomes fast and strong when the capillary number varies from $C_a = 5$ to $C_a = 30$ (Fig. 3(b)). In both cases $C_n = 0.2$ and $C_n = 0.4$, the concentration of platelet near wall is roughly same for $C_a = 30$ and $C_a = 70$, because $C_a = 30$ is sufficient to ensure the maximum of margination. These observations are in line with Krüger et al [30]. In their study, they studied the dependency of the platelet's margination on the channel diameter and capillary number. They used three-dimensional simulations with deformable and nearly rigid particles mimicking RBCs and platelets respectively. They figured out that the margination is fast for high capillary number with channel diameter up to $20\mu m$. However, there is no strong difference in platelet margination in the case of channel diameter greater than $20\mu m$. Our two dimensional model of RBC, which takes into account the RBC membrane proprieties without cytoskeleton, capture these features and constitutes a interesting test before embarking on the main question of this study.

B. The importance of wall lift on platelet margination

The aim of this section is to highlight the importance of the migration due to the walls (named lift) in the process of margination.Generally, the cross-streamline migration of RBCs can be due both to the presence of bounding walls as well as to to the flow curvature[9]. The case of vesicle in a semi-bounded channel was investigated by Kaoui et al[28]. As a conclusion, they found that the lift due to the presence of the wall dominates over that due to flow curvature. A more systematic study by Nix et al[47] showed that the wall lift force often dominates, except for high enough viscosity contrast ($\lambda = 5$) where the two forces become of comparable order, provided that the cell is far away from the wall (at a distance of about 20 times the radius); for smaller distances the wall lift dominates. Note also that far away from the center, and fotiori, in the vicinity of the wall the flow field is rather linear, so that we expect the wall lift force to be the dominant factor in creating the CFL.

The results of this section will be useful in interpreting the effect of adhesion energy on the margination process.

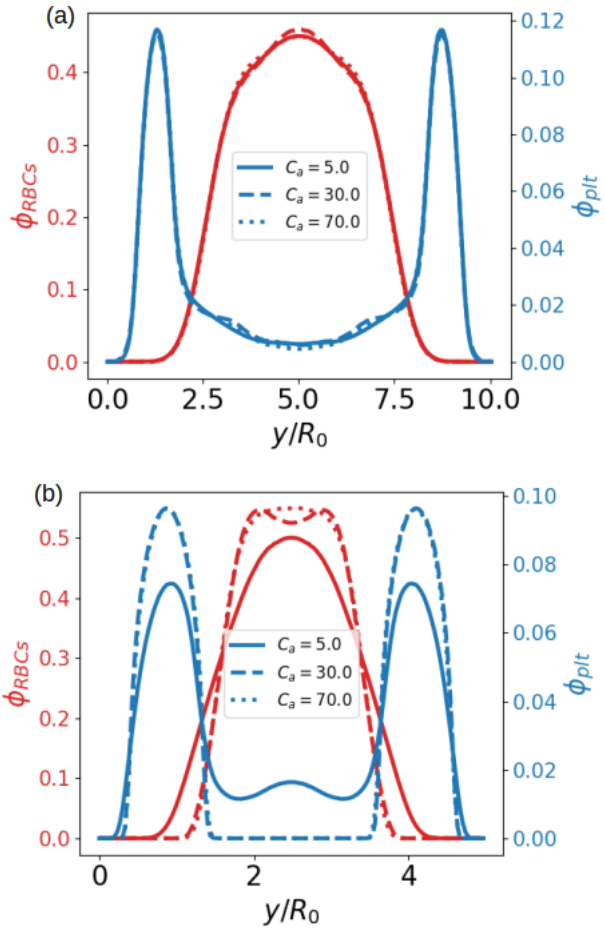

FIG. 3. Time-averaged concentration profile of platelets (ϕ_{plt}) and RBCs (ϕ_{RBCs}) for $C_a = 5, 30, 70$, $\lambda = 1$, $C_n = 0.2$, $\phi = 0.20$, and $\bar{\varepsilon} = 0$. (a) $C_n = 0.2$; (b) $C_n = 0.4$. The dotted, dashed and solid Blue/Red lines represent the time-averaged concentrations profile of platelets and RBCs respectively. The dotted and dashed blue lines in Fig. (b) are superposed.

It is known that at low viscosity contrast value, vesicles under shear flow undergo tank-treading (TT) dynamics (the vesicle adopts a fixed orientation and the membrane rotates around the inner fluid in a tank-tread fashion), whereas at high enough value of viscosity contrast vesicles exhibit tumbling (TB) dynamics where the vesicle rotate as a rigid body[24, 27]. The critical value of the viscosity contrast that corresponds to the transition between tank-treading and tumbling depends on confinement and reduced area [44]. In the TT regime, and at low enough viscosity contrast, the angle made by the vesicle with the flow direction is large enough, so that there is a strong upstream-downstream asymmetry, leading to a large enough lift. When the viscosity contrast is close to the critical value for TT-TB transition, the vesicle orientation angle is close to zero, leading to a a very small upstream-downstream asymmetry, and thus to a very small lift (owing to the Stokes reversibility upon time reversal). In the TB regime, on an average over a period of TB, there is upstream-downstream symmetry, and thus the lift is almost zero. Thus, the lift (migration due to wall) critically depends on the type of dynamics. Since lift is small in the TB regime, it is natural to expect a decline of platelet margination in this regime. Actually, Krüger et *al.*[30] have found that in the TT regime the margination is significantly stronger than in the TT regime. It has also been reported that decreasing viscosity contrast enhance [54]. Here we stress that the key point that influences margination is not TT or TB in itself, but rather the evolution of the lift due to walls, as will be seen below.

We performed simulations by fixing the confinement and the capillary number to $C_n = 0.2$ and $C_a = 30$. We selected three values of viscosity contrasts, two for which a single vesicle undergoes TT ($\lambda = 1$ and $\lambda = 5$) and one value for which a single vesicle undergoes TB ($\lambda = 10$). The main difference between the cases $\lambda = 1$ and $\lambda = 5$ is that for $\lambda = 1$ the vesicle inclination angle is significantly larger than that corresponding to $\lambda = 5$.

We investigated the platelet margination for the three values of λ.

Figure 4 illustrates more clearly the dependence of the margination phenomenon on λ. It is seen that margination is quite ample for $\lambda = 1$, as compared to the cases $\lambda = 5, 10$. Notably, the distributions of platelets for $\lambda = 5$ and $\lambda = 10$ are quite close to each other despite the fact for $\lambda = 5$ the vesicle exhibits TT whereas for $\lambda = 10$ it undergoes TB. In conclusion, the margination effect is not associated to TT or TB, but is rather dictated by the importance of lift. As mentioned above, for both $\lambda = 5$ and 10 the lift is small, but in the first case it is due to the small orientation angle of the vesicle with the flow direction (leading to a weak upstream-down asymmetry), whereas in the second case it is due to the fact that in the TB regime (and over one TB period) the upstream-downstream asymmetry is very weak (implying a small lift). Note that the platelet concentration increases in the RBCs core region for $\lambda = 5, 10$, as shown in Fig. 4. This is attributed to a decrease of lift force, which results in a decrease of CFL, leaving thus more space in the core region where platelets can be trapped. This implies that platelet margination is reduced.

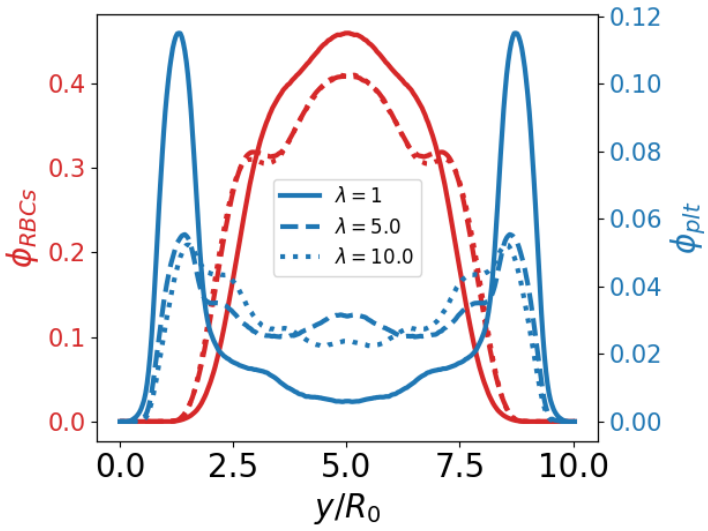

FIG. 4. Time-averaged concentration profile of platelets and RBCs for $\lambda = 1, 5, 10$, $C_a = 30$, $C_n = 0.2$, $\phi = 0.20$, and $\bar{\varepsilon} = 0$.The dashed and solid Blue/Red lines present the Time-averaged concentration profile of Platelets/RBCs for $\lambda = 1$ and $\lambda = 10$ respectively.

C. The effect of the adhesion energy between red blood cells on platelet margination

In-vivo, fibrinogen is believed to be the main actor for adhesion between RBCs. In the case of diabetes, pregnancy and cardiac diseases, the concentration of fibrinogen is higher than the usual physiological concentration [20], which should enhance the aggregation process[8, 41]. In this section we analyze the effect of the adhesion energy between RBCs on platelets margination.

Figure 5, shows snapshots of RBCs and platelets configurations in the absence and in the presence of adhesion energy between RBCs. The snapshots are taken at the early stage of simulation and at the end of the simulation. Simulation time t is scaled by τ_c ($\tau_c = \eta_{ex} R_0^3/k$) which is the typical time needed for the vesicle to return to its equilibrium shape after cessation of flow.

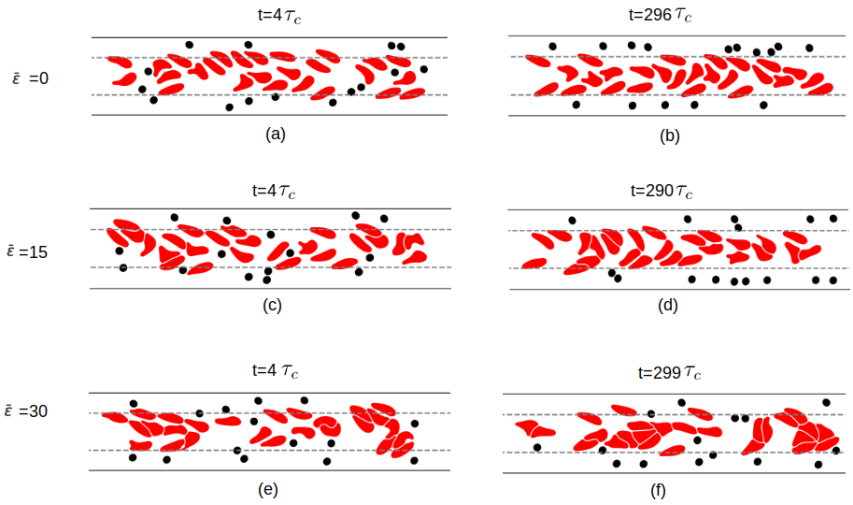

FIG. 5. Snapshots of simulation domain with both RBCs and platelets for different values of adhesion energy between RBCs $\bar{\varepsilon}$. The cell free layer is denoted by horizontal dashed line.

A close inspection of the platelet concentration profile reveals a non trivial behavior (see Fig. 6). For varying hematocrit levels, a remarkable feature is that a moderate adhesion energy among RBCs ($\bar{\varepsilon} = 15$, corresponding to the lower range of physiological adhesion energy; see Table I) increases the platelet margination. This increase is quite significant for $\phi = 0.2$ than for higher hematocrits.. More precisely, for $\phi = 0.2$, the platelet concentration in the cell-free layer is increased by about 20% in the presence of modest adhesion, $\bar{\varepsilon} = 15$, as compared to the free-adhesion case. This increase is , however, smaller for $\phi = 0.3$ and $\phi = 0.4$. We will examine in section IV the behaviour in microcirculation where hematocrit is in the range $5 - 20\%$[7, 29, 34, 38], and we will see that the effect of adhesion energy on margination is even ampler. When the adhesion energy among RBCs is significantly increased, there is a decline in platelet margination (Fig. 6). In summary, the platelet margination is non monotonic with respect to the adhesion energy between RBCs. Figure 7, illustrates the time-averaged concentration profile of RBCs for different hematocrit levels, $\phi = 0.20, 0.30, 0.40$. For a modest increase of adhesion energy from $\bar{\varepsilon} = 0$ to $\bar{\varepsilon} = 15$ RBCs tend to accumulate more towards the center (green line in Fig. 7) as compared to the case without adhesion energy (blue line in Fig. 7). The fact that RBCs accumulate towards the center for a moderate adhesion energy is correlated with the increase of margination discussed above. Increasing further the adhesion energy leads to more accumulation of RBCs towards the periphery. This leads to a decrease of margination. In order to quantify these effects we have calculated the width of the cell-free layer (CFL) as a function of adhesion energy. Figure 8 confirms the results reported in Fig. 7. There are different ways to define the CFL. Here we follow the method of [63]. We first calculate the time and space (along x) average concentration profile of RBCs, which depends on y only, $\phi_{RBCs}(y)$. Then we integrate this function over y from 0 to a certain y starting from the bottom channel wall and normalize it with the total integrated value over the entire channel width. Then, we define the cell-free layer boundary as the location y where only 5% of the total RBC concentration is present from the lower channel wall to that point.

The CFL shows a non monotonic behavior (Fig. 8) as a function of the adhesion energy for both hematocrit $\phi = 0.20$ (Fig. 8a) and $\phi = 0.40$ (Fig. 8b) . This non monotonic behavior is correlated with the non monotonic platelets margination reported in Fig. 6. The platelet margination mostly occurs after the cell free layer (CFL) has fully developed [15]. Platelets are trapped in the CFL during their first visit [64]. For different channel widths we investigated the effect of the adhesion energy between RBCs on cell free layer thickness Fig. 8. For hematocrit $\phi = 0.20$, capillary number $C_a = 30$ and for different channel widths W, the CFL thickness is found to decrease with

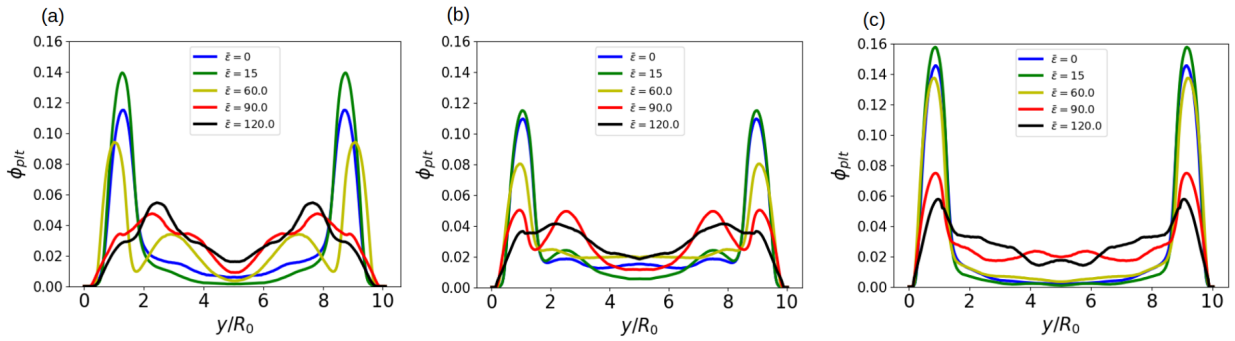

FIG. 6. Time-averaged concentration profile of platelets for (a) $\phi = 0.20$; (b) $\phi = 0.30$; (c) $\phi = 0.40$. $\bar{\varepsilon} = 0, 15, 60, 90, 120$, $\lambda = 1$, $C_n = 0.2$ and $C_a = 30$.

increased adhesion energy after an optimum value of $\bar{\varepsilon} = 15$. In addition to the weak number of RBCs undergoing tank treading (which facilitate the transport of platelets into the CFL) in case of high adhesion energy between RBCs, the CFL thickness is smaller. Therefor, platelets come back to the RBC core before reaching the CFL. According to Figs. 7-6, the increase of adhesion energy between RBCs decreases the tendency of platelets to move towards the walls. The increase of RBCs aggregation (due to an increase of adhesion energy between RBC) decreases the number of cells in the middle of the channel as well as free RBCs undergoing tank-treading. This section results validates the previous section results about the importance of RBCs lateral migration for platelets margination.

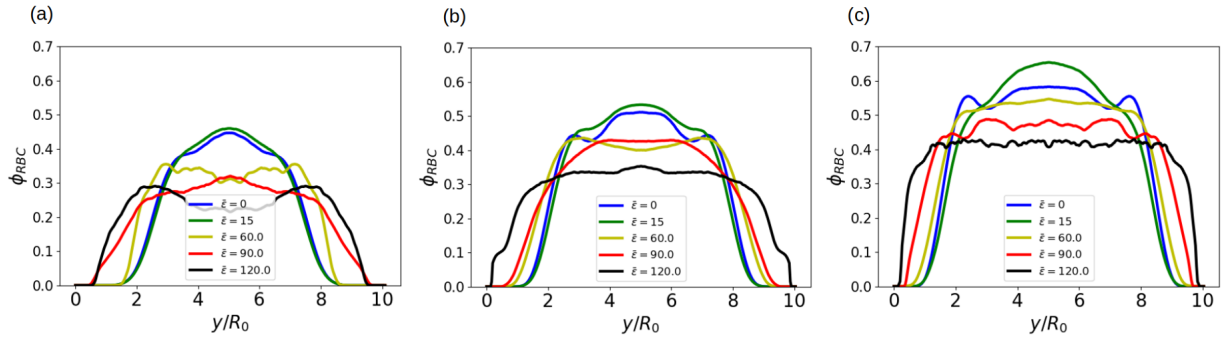

FIG. 7. Time-averaged concentration profile of RBCs for (a) $\phi = 0.20$; (b) $\phi = 0.30$; (c) $\phi = 0.40$. $\bar{\varepsilon} = 0, 15, 60, 90, 120$, $\lambda = 1$, $C_n = 0.2$ and $C_a = 30$.

We have investigated the role of the capillary number on platelet margination, as shown in Fig. 9. It is seen that increasing the capillary number from $C_a = 5$ to $C_a = 70$ notably enhances platelet margination in the presence of adhesion among RBCs. In contrast, when $\bar{\varepsilon} = 0$, the concentration of platelets near the wall is quite insensitive to the capillary number. For both $C_a = 30$ and $C_a = 70$ we observe the non monotonic behavior of platelet margination. When C_a is large enough in comparison to unity most of cells reach their maximal deformation (saturation due to membrane inextensibility. When C_a is small enough ($C_a = 5$ in the studied case, which corresponds to speed far below those encountered in microcirculation), the lift is small (and so is the CFL) leading to a moderate margination. In addition even for a small adhesion energy the aggregate do not significantly break, and provides more space in the core region to trap platelets. Overall, the platelet margination decreases and remains weakly sensitive to an increase of adhesion energy. Finally, Fig. 10 compares platelets trajectories for two values of adhesion energy between RBCs, respectively $\bar{\varepsilon} = 0$ and $\bar{\varepsilon} = 90$. In the absence of adhesion energy, platelets migrate rapidly and the majority reach the outer layer after traveling an average distance of $400\mu m$, but, for $\bar{\varepsilon} = 90$, platelets stay in the vessel core during their travel through the vessel.

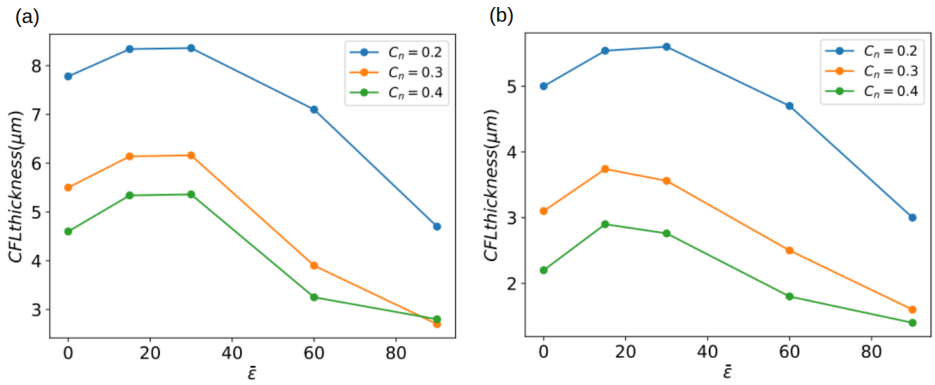

FIG. 8. Cell free layer thickness as function of adhesion energy $\bar{\varepsilon}$ for all investigated confinement C_n for (a) $\phi = 0.20$; (b) $\phi = 0.40$.

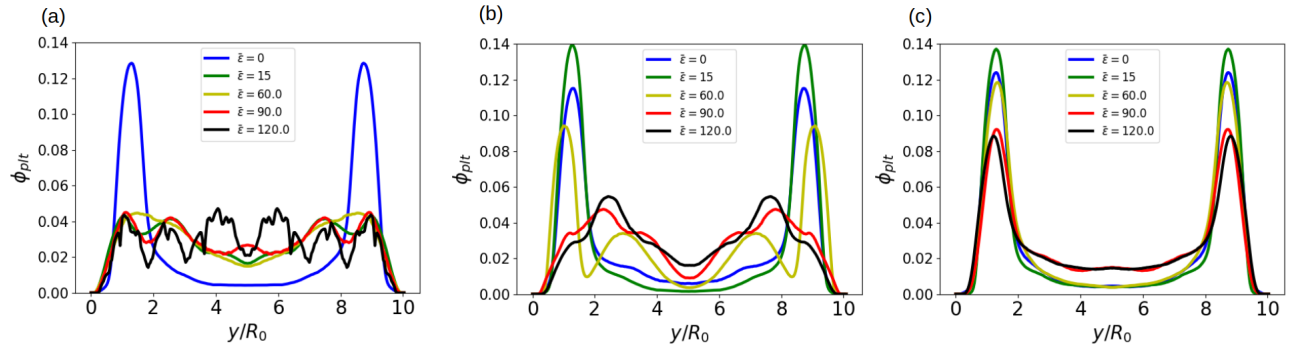

FIG. 9. Time-averaged concentration profile of platelets for (a) $C_a = 5$; (b) $C_a = 30$; (c) $C_a = 70$. $\bar{\varepsilon} = 0, 15, 60, 90, 120$, $\lambda = 1$, $C_n = 0.2$ and $\phi = 0.20$.

IV. FOCUS ON MICROCIRCULATION WITH A REALISTIC VISCOSITY CONTRAST

In this section we summarize our results relevant for hematocrit in microcirculation, by adopting a viscosity contrast inspired by that of RBC, namely $\lambda = 5$. Indeed, in microcirculation hematocrit lies within 5%-20% [7, 29, 34, 38] range. We have thus run simulations with $\phi = 0.1, 0.15, 0.2$ and $\lambda = 5$. We have also explored two typical values of flow strength, measured by the capillary number , namely $C_a = 30$ and $C_a = 70$. Figure 11 shows the platelet profiles and the RBC profiles for $C_a = 30$ for $\phi = 0.1, 0.15, 0.2$ and $\lambda = 5$. Figure 12 shows the results for $C_a = 70$. Both for $C_a = 30$ and $C_a = 70$ we see a non monotonic behavior of the platelet profile as a function of adhesion energy. At small and moderate energies the platelet profile peak is boosted by adhesion energy.

A more precise way to show the effect of the adhesion energy on platelet margination is to plot the integrated platelet concentration in the CFL. The result is shown in Fig.13 for both $C_a = 30$ and $C_a = 70$. In the case of $C_a = 30$, except for $\phi = 0.1$ where the boost is moderate, the impact of adhesion is quite significant for $\phi = 0.15$ and $\phi = 0.2$. In the first case there is about 30% platelet in the CFL in the absence of adhesion, a value that reaches about 50% for adhesion energy $\bar{\epsilon} = 15$. In the second case the platelet proportion in the CFL goes from about 35% in the absence of adhesion to about 58% for $\bar{\epsilon} = 15$. For higher $C_a = 70$ the increase of platelet in CFL is even stronger, going (for $\phi = 0.1$) from 33% (in the absence of adhesion) to 53% for $\bar{\epsilon} = 15$, and (for $\phi = 0.15$) from 30% to about 77% for $\bar{\epsilon} = 90$. These results clearly show an important impact of adhesion energy on platelet margination.

A peculiar behavior is observed for the case of $C_a = 70$ where the platelet concentration in the CFL (Fig. 13) shows a minimum at a certain adhesion energy and increases again at higher adhesion energy. Note the value of the platelet concentration still remains smaller or close to that in the absence of adhesion energy. To dig further into this effect we focus on the case $\phi = 0.15$ and $C_a = 70$ where the platelet concentration in the CFL reaches a minimum for adhesion energy $\bar{\epsilon} = 90$ and then increases to a relatively larger value at higher adhesion energy $\bar{\epsilon} = 120$ (orange curve in Fig.13). A snapshot. of the cell configuration for each case is represented in Fig.14 . We see there that for $\bar{\epsilon} = 90$ the aggregate are quite rounded with large separation among aggregates, leaving thus ample free spce allowing

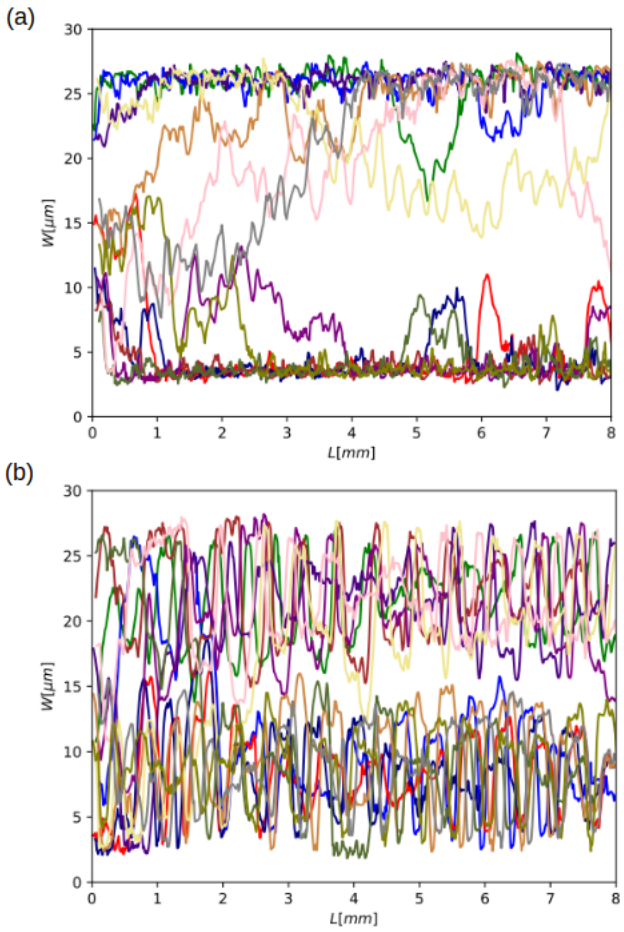

FIG. 10. The Platelets trajectories (a) $\bar{\varepsilon} = 0$; (b) $\bar{\varepsilon} = 90$. $C_a = 30$, $\phi = 0.20$, $\lambda = 1$, $C_n = 0.2$.

to platelet to explore the central region of the channel. For $\bar{\epsilon} = 120$ larger aggregates form and, due to confinement, the aggregate are more elongated leaving less free space for platelet to explore the central region. As a consequence due to this geometric configuration the margination is relatively higher for a higher adhesion energy.

V. DISCUSSION

The margination of platelet can be viewed as follows. Suppose we have initially a random distribution of RBCs and platelets within the channel. When the flow is applied, RBCs have a tendency to be pushed away from the walls thanks to the lift mechanism, leaving a CFL close to the walls. At the same time platelets (as being rigid) do not experience a significant lift. The platelets which were located initially in the core region, will undergo collisions against RBCs and undergo a diffusion-like process (of hydrodynamic origin). This diffusion will cause platelets to spread across streamlines. Once a platelet reaches the CFL it will be trapped there, owing to the absence of a significant lift. This process is efficient for a large enough hematocrit, as reported in Ref.[30]).

For a modest adhesion energy (middle panels in Fig. 5) some RBCs, initially at the extreme peripheries, will be weakly attracted by some RBCs setting in the next files of RBCs, leading to a small fraction of small clusters (while there are single many RBCs), like RBCs doublets (see middle panel in Fig. 5). This increases the CFL width. This will naturally enhance the margination process. For a larger adhesion energy (see lower panel in Fig. 5, large enough clusters form. This has two consequences: (i) the clusters often rotate (as described in details for doublets in Ref. [3]), and as for a tumbling RBC, the lift is reduced, leading to a reduction of the CFL, (ii) the formation of many clusters in the core region, increases free-cell spaces, allowing thereby platelets to visit more easily these regions, even for those initially in the CFL, thanks to collision with RBCs clusters. These two mechanisms lead to a decline of

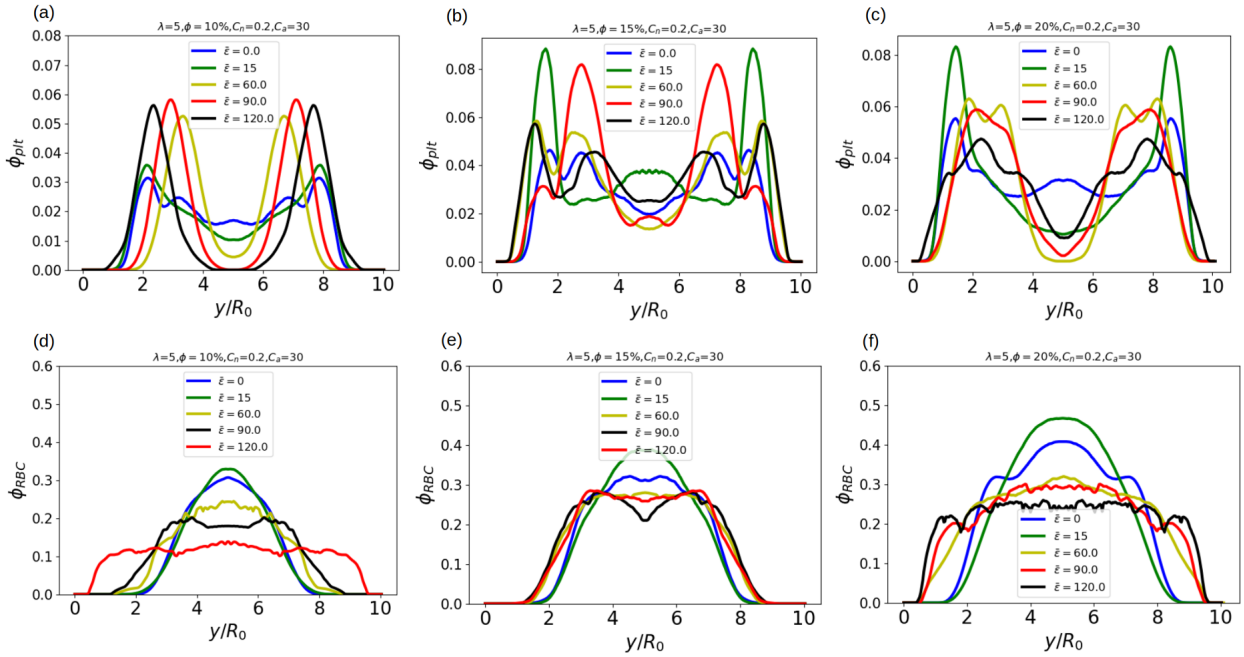

FIG. 11. Top: the platelet profiles, and Bottom: RBC profiles for $C_a = 30$, $\lambda = 5$ and for different adhesion energies.

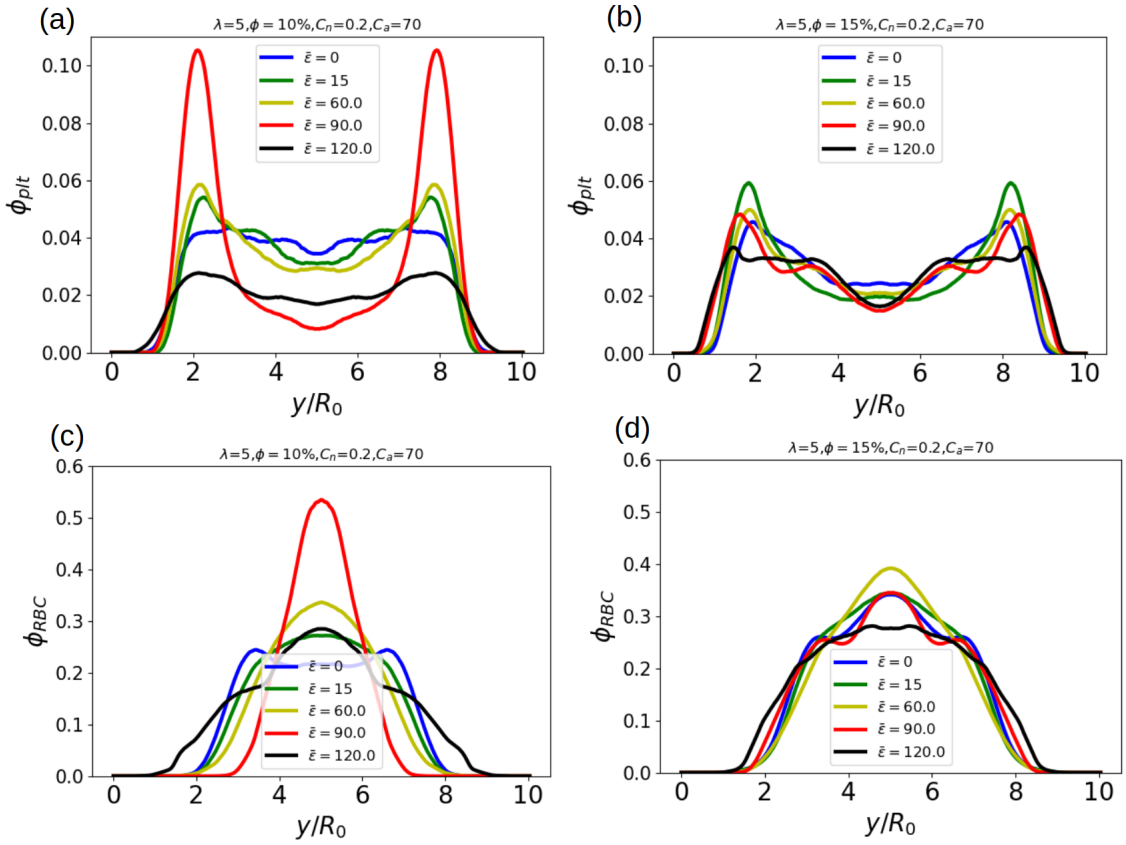

FIG. 12. Top: the platelet profiles, and Bottom: RBC profiles for $C_a = 70$, $\lambda = 5$ and for different adhesion energies.

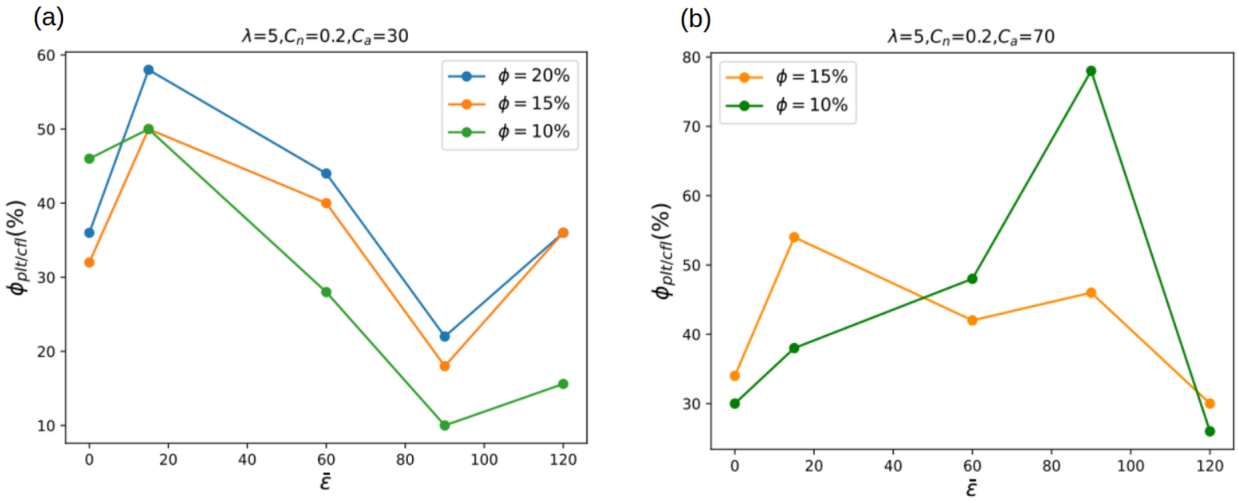

FIG. 13. Top: the integrated platelet profile for $C_a = 30$, $\lambda = 5$ and different hematocrits as a function of adhesion energy.

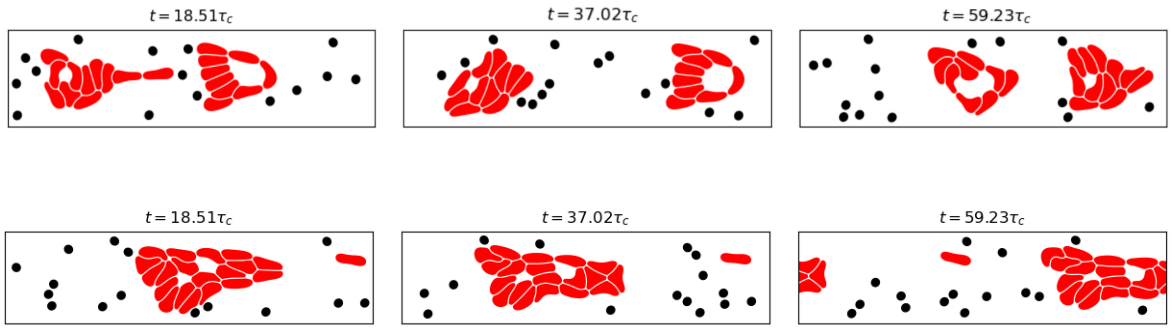

FIG. 14. Snapshots of RBCs configuration for $\bar{\varepsilon} = 90$ (top) and $\bar{\varepsilon} = 120$ (bottom). $\phi = 0.15$, $C_a = 70$, $\lambda = 5$, $C_n = 0.2$.

platelet margination.

There are several diseases which are known to lead to robust aggregation among RBCs. A well known situation is that encountered in diabetes mellitus [20]. The precise origin of enhanced aggregation for patients suffering diabetes is not yet completely elucidated, albeit the formation of robust clusters of RBCs is beyond any doubt. It is well documented that these patients suffer from uncontrolled bleeding for which several factors have been reported in [36], such as coagulation disorders, hypofibrinolysis and changes in platelet number and activation . It will be an important task for future investigations to elucidate if the mechanisms reported here may contribute efficiently to uncontrolled bleeding for diabetic patients. There are, however, several cautions. It has been reported that the channel length must be of the order of 300 μm before full platelet margination to take place [54]. Those studies, as well as the present one, pertain to microvascular networks, in which the vessel length rarely exceed this length, before meeting a bifurcation. Several studies have explored the process of platelets and other blood cells marginating within bifurcations [4, 45, 48]. Bächer et al. [4] showed that a bifurcation does not significantly impact platelet margination, provided that the initial configuration corresponds to platelets which are close to the channel walls in the mother branch. In contrast, a confluence is found to reduce the margination[4]. Noguchi et al[48]reported that a distance of 5 mm is necessary after a confluence for platelets to marginate again[48]. It is important to study the margination process in a realistic network (containing bifurcations and confluences) where platelets are initially randomly positioned in a mother vessel, and analyze the influence of various parameters (flow strength, hematocrit, RBC aggregation, viscosity contrast) that could affect platelet behavior.

VI. CONCLUSION

We have investigated the platelet margination in a simple straight channel in the presence of adhesion energy among RBCs. We have first clarified the role of the lift in the process of margination, by showing that even if RBCs undergo tank-treading (TT) the platelet margination an be as weak as in the case when they exhibit tumbling. If the orientation angle of the RBCs is weak enough the effect of margination can be as weak as in the case for a tumbling (TB) cell. This is attributed to the weak upstream-downstream asymmetry, and not to the fact that a cell is in the TT or TB regime. We have then investigated the role of adhesion in the process of margination. A remarkable feature discovered here is that the margination is non monotonic with respect to the adhesion energy. A modest adhesion energy, as encountered under normal physiological conditions, is found to boost the margination process, whereas a strong enough adhesion leads to a decline of margination. We have provided an intuitive explanation to this behavior. As highlighted in the previous section, the typical channel length for a complete margination of platelets is several hundreds of micrometers, a length which generally exceeds that of vessels in microvascular networks. In order to have a complete picture of margination in vivo a simulation in a realistic vascular network is necessary. Finally, our simulation has a limitation since it is based on 2D, which serves at least as a guide. While it has been shown in different works that the 2D model captures several features observed in 3D [2, 3, 19, 22, 23, 33, 42], a full 3D simulation is necessary before drawing definite conclusive answers. It is hoped to investigated this matter further in a future work.

ACKNOWLEDGEMENTS

We acknowledge financial support from CNES (Centre National d'Etudes Spatiales), and the French-German University Programme "Living Fluids" (Grant CFDA-Q1-14). M.D. and C.M. acknowledge funding by the Marie Skodowska-Curie grant agreement no. 860436, EVIDENCE. The simulations were performed on the Cactus cluster of the CIMENT infrastructure, which is supported by the Rhône-Alpes region (Grant No. CPER07_13 CIRA).

[1] PA Aarts, SA Van Den Broek, Gerrit W Prins, GD Kuiken, Jan J Sixma, and Robert M Heethaar. Blood platelets are concentrated near the wall and red blood cells, in the center in flowing blood. *Arteriosclerosis: An Official Journal of the American Heart Association, Inc.*, 8(6):819–824, 1988.

[2] Mehdi Abbasi, Alexander Farutin, Hamid Ez-Zahraouy, Abdelilah Benyoussef, and Chaouqi Misbah. Erythrocyte-erythrocyte aggregation dynamics under shear flow. *Physical Review Fluids*, 6(2):023602, 2021.

[3] Mehdi Abbasi, Alexander Farutin, Abdessamad Nait-Ouhra, Hamid Ez-Zahraouy, Abdelilah Benyoussef, and Chaouqi Misbah. Dynamics and rheology of a single two-dimensional multilobe vesicle in a confined geometry. *Physical Review Fluids*, 7(9):093603, 2022.

[4] Christian Bächer, Alexander Kihm, Lukas Schrack, Lars Kaestner, Matthias W Laschke, Christian Wagner, and Stephan Gekle. Antimargination of microparticles and platelets in the vicinity of branching vessels. *Biophysical journal*, 115(2):411–425, 2018.

[5] Christian Bächer, Lukas Schrack, and Stephan Gekle. Clustering of microscopic particles in constricted blood flow. *Physical Review Fluids*, 2(1):013102, 2017.

[6] Rocco Barazzoni, Michela Zanetti, G Davanzo, E Kiwanuka, P Carraro, A Tiengo, and P Tessari. Increased fibrinogen production in type 2 diabetic patients without detectable vascular complications: correlation with plasma glucagon concentrations. *The Journal of Clinical Endocrinology & Metabolism*, 85(9):3121–3125, 2000.

[7] Joseph Boyle III. Microcirculatory hematocrit and blood flow. *Journal of theoretical biology*, 131(2):223–229, 1988.

[8] Matthias Brust, Othmane Aouane, Marine Thiébaud, Daniel Flormann, Claude Verdier, Lars Kaestner, MW Laschke, Hassib Selmi, Abdellilah Benyoussef, Thomas Podgorski, et al. The plasma protein fibrinogen stabilizes clusters of red blood cells in microcapillary flows. *Scientific reports*, 4(1):4348, 2014.

[9] Lionel Bureau, Gwennou Coupier, and Thomas Salez. Lift at low reynolds number. *The European Physical Journal E*, 46(11):111, 2023.

[10] K Buxbaum, E Evans, and DE Brooks. Quantitation of surface affinities of red blood cells in dextran solutions and plasma. *Biochemistry*, 21(13):3235–3239, 1982.

[11] Hung-Yu Chang, Alireza Yazdani, Xuejin Li, Konstantinos AA Douglas, Christos S Mantzoros, and George Em Karniadakis. Quantifying platelet margination in diabetic blood flow. *Biophysical journal*, 115(7):1371–1382, 2018.

[12] Shu Chien and Kung-ming Jan. Ultrastructural basis of the mechanism of rouleaux formation. *Microvascular research*, 5(2):155–166, 1973.

[13] Viviana Clavería, Othmane Aouane, Marine Thiébaud, Manouk Abkarian, Gwennou Coupier, Chaouqi Misbah, Thomas John, and Christian Wagner. Clusters of red blood cells in microcapillary flow: hydrodynamic versus macromolecule induced interaction. *Soft Matter*, 12(39):8235–8245, 2016.

[14] Gonçalo Coutinho, Ana S Moita, Massimiliano Rossi, and António LN Moreira. Experimental perspective on the mechanisms for near-wall accumulation of platelet-size particles in pressure-driven red blood cell suspension flows. *Physical Review Fluids*, 8(10):103101, 2023.

[15] Lindsay M Crowl and Aaron L Fogelson. Computational model of whole blood exhibiting lateral platelet motion induced by red blood cells. *International journal for numerical methods in biomedical engineering*, 26(3-4):471–487, 2010.

[16] Benjamin Czaja, Mario Gutierrez, Gábor Závodszky, David de Kanter, Alfons Hoekstra, and Omolola Eniola-Adefeso. The influence of red blood cell deformability on hematocrit profiles and platelet margination. *PLoS Computational Biology*, 16(3):e1007716, 2020.

[17] Dmitry A Fedosov, Julia Fornleitner, and Gerhard Gompper. Margination of white blood cells in microcapillary flow. *Physical review letters*, 108(2):028104, 2012.

[18] Dmitry A Fedosov and Gerhard Gompper. White blood cell margination in microcirculation. *Soft matter*, 10(17):2961–2970, 2014.

[19] Daniel Flormann, Othmane Aouane, Lars Kaestner, Christian Ruloff, Chaouqi Misbah, Thomas Podgorski, and Christian Wagner. The buckling instability of aggregating red blood cells. *Scientific reports*, 7(1):1–10, 2017.

[20] Patricia Foresto, MABEL D Arrigo, Larisa Carreras, Raul Etchepare Cuezzo, Juana Valverde, and Rodolfo Rasia. Evaluation of red blood cell aggregation in diabetes by computarized image analysis. *MEDICINA-BUENOS AIRES-*, 60(5; PART 1):570–572, 2000.

[21] Harry L Goldsmith and Samira Spain. Margination of leukocytes in blood flow through small tubes. *Microvascular research*, 27(2):204–222, 1984.

[22] B Kaoui, N Tahiri, T Biben, H Ez-Zahraouy, A Benyoussef, G Biros, and C Misbah. Complexity of vesicle microcirculation. *Physical Review E*, 84(4):041906, 2011.

[23] Badr Kaoui, George Biros, and Chaouqi Misbah. Why do red blood cells have asymmetric shapes even in a symmetric flow? *Physical review letters*, 103(18):188101, 2009.

[24] Badr Kaoui, Alexander Farutin, and Chaouqi Misbah. Vesicles under simple shear flow: Elucidating the role of relevant control parameters. *Physical Review E*, 80(6):061905, 2009.

[25] Badr Kaoui and Jens Harting. Two-dimensional lattice boltzmann simulations of vesicles with viscosity contrast. *Rheologica Acta*, 55(6):465–475, 2016.

[26] Badr Kaoui, Jens Harting, and Chaouqi Misbah. Two-dimensional vesicle dynamics under shear flow: Effect of confinement. *Phys. Rev. E*, 83:066319, Jun 2011.

[27] Badr Kaoui, Ruben JW Jonk, and Jens Harting. Interplay between microdynamics and macrorheology in vesicle suspensions. *Soft Matter*, 10(26):4735–4742, 2014.

[28] Badr Kaoui, GH Ristow, Isabelle Cantat, Chaouqi Misbah, and Walter Zimmermann. Lateral migration of a two-dimensional vesicle in unbounded poiseuille flow. *Physical Review E*, 77(2):021903, 2008.

[29] BRUCE Klitzman and BRIAN R Duling. Microvascular hematocrit and red cell flow in resting and contracting striated muscle. *American Journal of Physiology-Heart and Circulatory Physiology*, 237(4):H481–H490, 1979.

[30] Timm Krüger. Effect of tube diameter and capillary number on platelet margination and near-wall dynamics. *Rheologica Acta*, 55(6):511–526, 2016.

[31] Timm Krüger, Stefan Frijters, Florian Günther, Badr Kaoui, and Jens Harting. Numerical simulations of complex fluid-fluid interface dynamics. *The European Physical Journal Special Topics*, 222(1):177–198, 2013.

[32] Timm Krüger, Fathollah Varnik, and Dierk Raabe. Efficient and accurate simulations of deformable particles immersed in a fluid using a combined immersed boundary lattice boltzmann finite element method. *Computers & Mathematics with Applications*, 61(12):3485–3505, 2011.

[33] Luca Lanotte, Johannes Mauer, Simon Mendez, Dmitry A Fedosov, Jean-Marc Fromental, Viviana Claveria, Franck Nicoud, Gerhard Gompper, and Manouk Abkarian. Red cells dynamic morphologies govern blood shear thinning under microcirculatory flow conditions. *Proceedings of the National Academy of Sciences*, 113(47):13289–13294, 2016.

[34] Guansheng Li, Ting Ye, Zehong Xia, Sitong Wang, and Ziwei Zhu. Analysis and prediction of hematocrit in microvascular networks. *International Journal of Engineering Science*, 191:103901, 2023.

[35] Lujuan Li, Shuo Wang, Keqin Han, Xiaojing Qi, Shuhao Ma, Li Li, Jun Yin, Dechang Li, Xuejin Li, and Jin Qian. Quantifying shear-induced margination and adhesion of platelets in microvascular blood flow. *Journal of Molecular Biology*, 435(1):167824, 2023.

[36] Xiaoling Li, Nina C Weber, Danny M Cohn, Markus W Hollmann, J Hans DeVries, Jeroen Hermanides, and Benedikt Preckel. Effects of hyperglycemia and diabetes mellitus on coagulation and hemostasis. *Journal of clinical medicine*, 10(11):2419, 2021.

[37] TC Lim. The relationship between lennard-jones (12-6) and morse potential functions. *ZEITSCHRIFT FUR NATURFORSCHUNG SECTION A-A JOURNAL OF PHYSICAL SCIENCES*, 58(11):615–617, NOV 2003.

[38] Herbert H Lipowsky, Shunichi Usami, and Shu Chien. In vivo measurements of apparent viscosity and microvessel hematocrit in the mesentery of the cat. *Microvascular research*, 19(3):297–319, 1980.

[39] Yaling Liu and Wing Kam Liu. Rheology of red blood cell aggregation by computer simulation. *Journal of Computational Physics*, 220(1):139–154, 2006.

[40] Wieland Marth, Sebastian Aland, and Axel Voigt. Margination of white blood cells: a computational approach by a hydrodynamic phase field model. *Journal of fluid mechanics*, 790:389–406, 2016.

[41] Anastasia Maslianitsyna, Petr Ermolinskiy, Andrei Lugovtsov, Alexandra Pigurenko, Maria Sasonko, Yury Gurfinkel, and Alexander Priezzhev. Multimodal diagnostics of microrheologic alterations in blood of coronary heart disease and diabetic patients. *Diagnostics*, 11(1):76, 2021.

[42] Johannes Mauer, Simon Mendez, Luca Lanotte, Franck Nicoud, Manouk Abkarian, Gerhard Gompper, and Dmitry A Fedosov. Flow-induced transitions of red blood cell shapes under shear. *Physical review letters*, 121(11):118103, 2018.

[43] Alexander E Moskalensky, Maxim A Yurkin, Artem R Muliukov, Alena L Litvinenko, Vyacheslav M Nekrasov, Andrei V Chernyshev, and Valeri P Maltsev. Method for the simulation of blood platelet shape and its evolution during activation. *PLoS computational biology*, 14(3):e1005899, 2018.

[44] Abdessamad Nait-Ouhra, Alexander Farutin, Hamid Ez-Zahraouy, Abdelilah Benyoussef, and Chaouqi Misbah. Rheology of a confined vesicle suspension. *Physical Review Fluids*, 4(10):103602, 2019.

[45] Bumseok Namgung, Yan Cheng Ng, Hwa Liang Leo, Joseph M Rifkind, and Sangho Kim. Near-wall migration dynamics of erythrocytes in vivo: effects of cell deformability and arteriolar bifurcation. *Frontiers in physiology*, 8:307025, 2017.

[46] Björn Neu and Herbert J Meiselman. Depletion-mediated red blood cell aggregation in polymer solutions. *Biophysical journal*, 83(5):2482–2490, 2002.

[47] S Nix, Y Imai, and T Ishikawa. Lateral migration of a capsule in a parabolic flow. *Journal of biomechanics*, 49(11):2249–2254, 2016.

[48] Akira Noguchi, Yuki Tange, Tomoaki Itano, and Masako Sugihara-Seki. Margination of platelet-sized particles in red blood cell suspensions flowing through a y-shaped confluence microchannel. *Fluid Dynamics Research*, 55(3):035506, 2023.

[49] Dongig Oh, Satoshi Ii, and Shu Takagi. Numerical study of particle margination in a square channel flow with red blood cells. *Fluids*, 7(3):96, 2022.

[50] Charles S Peskin. The immersed boundary method. *Acta numerica*, 11:479–517, 2002.

[51] Jordan S Pober and William C Sessa. Evolving functions of endothelial cells in inflammation. *Nature Reviews Immunology*, 7(10):803–815, 2007.

[52] Qin M Qi and Eric SG Shaqfeh. Theory to predict particle migration and margination in the pressure-driven channel flow of blood. *Physical review fluids*, 2(9):093102, 2017.

[53] Qin M Qi and Eric SG Shaqfeh. Time-dependent particle migration and margination in the pressure-driven channel flow of blood. *Physical Review Fluids*, 3(3):034302, 2018.

[54] Daniel A Reasor, Marmar Mehrabadi, David N Ku, and Cyrus K Aidun. Determination of critical parameters in platelet margination. *Annals of biomedical engineering*, 41(2):238–249, 2013.

[55] Zaiyi Shen, Alexander Farutin, Marine Thiébaud, and Chaouqi Misbah. Interaction and rheology of vesicle suspensions in confined shear flow. *Physical Review Fluids*, 2(10):103101, 2017.

[56] Andrew P Spann, James E Campbell, Sean R Fitzgibbon, Armando Rodriguez, Andrew P Cap, Lorne H Blackbourne, and Eric SG Shaqfeh. The effect of hematocrit on platelet adhesion: experiments and simulations. *Biophysical journal*, 111(3):577–588, 2016.

[57] Patrick Steffen, Claude Verdier, and Christian Wagner. Quantification of depletion-induced adhesion of red blood cells. *Physical review letters*, 110(1):018102, 2013.

[58] Naoki Takeishi, Marco E Rosti, Yohsuke Imai, Shigeo Wada, and Luca Brandt. Haemorheology in dilute, semi-dilute and dense suspensions of red blood cells. *Journal of Fluid Mechanics*, 872:818–848, 2019.

[59] Jonathan N Thon and Joseph E Italiano. Platelets: production, morphology and ultrastructure. *Antiplatelet Agents*, pages 3–22, 2012.

[60] Arno W Tilles and Eugene C Eckstein. The near-wall excess of platelet-sized particles in blood flow: its dependence on hematocrit and wall shear rate. *Microvascular research*, 33(2):211–223, 1987.

[61] Victor WM van Hinsbergh. Endotheliumrole in regulation of coagulation and inflammation. In *Seminars in immunopathology*, volume 34, pages 93–106. Springer, 2012.

[62] Alireza Yazdani, Yixiang Deng, He Li, Elahe Javadi, Zhen Li, Safa Jamali, Chensen Lin, Jay D Humphrey, Christos S Mantzoros, and George Em Karniadakis. Integrating blood cell mechanics, platelet adhesive dynamics and coagulation cascade for modelling thrombus formation in normal and diabetic blood. *Journal of the Royal Society Interface*, 18(175):20200834, 2021.

[63] Xuewen Yin, Tancred Thomas, and Junfeng Zhang. Multiple red blood cell flows through microvascular bifurcations: cell free layer, cell trajectory, and hematocrit separation. *Microvascular research*, 89:47–56, 2013.

[64] Hong Zhao and Eric SG Shaqfeh. Shear-induced platelet margination in a microchannel. *Physical Review E*, 83(6):061924, 2011.

[65] Ou-Yang Zhong-Can and Wolfgang Helfrich. Bending energy of vesicle membranes: General expressions for the first, second, and third variation of the shape energy and applications to spheres and cylinders. *Physical Review A*, 39(10):5280, 1989.